Heat and Mass Transfer
https://doi.org/10.1007/s00231-021-03044-7

ORIGINAL

The combined effects of cobalt chromite nanoparticles and variable injection timing of preheated biodiesel and diesel on performance, combustion and emission characteristics of CI engine

Anbarasan Baluchamy[1] · Muralidharan Karuppusamy[1]

Received: 31 July 2020 / Accepted: 25 February 2021

Abstract

The performance, emission, and combustion characteristics of kapok methyl ester biodiesel in the base engine were analyzed. The kapok methyl ester oil is heated up to 110 °C employing a preheating method to reduce the fuel's viscosity and density. The preheated oil is blended with the base fuel (i.e., diesel) to make various fuel blends. Many research findings have shown that the B20 (i.e., 20% biodiesel and 80% diesel) blend reveals superior performance, emission, and combustion characteristics in the diesel engine. Preheated oil was mixed with cobalt chromite nanoparticles in the different dosages of 50 ppm, 100 ppm, 150 ppm, and 200 ppm, respectively. When using this biodiesel in a diesel engine, the oxide of nitrogen increases. To overcome this problem, the injection timing concept was used. The injection timing was varied by 19 crank angle degree (CAD) bTDC (Retardation), 23 CAD bTDC (Standard), and 27 CAD bTDC (Advanced). The brake thermal efficiency increased with the blends B20 with cobalt 200 ppm in Retardation by 7.2% as compared with the started ignition delay. The hydrocarbon and carbon monoxide decreased in the blends B20 with cobalt 200 ppm in Retardation by 37.86% and 41.66% as compared to the standard injection timing. The oxides of nitrogen and carbon monoxide of blend B20 with cobalt 50 ppm in Retardation decreased by 16.45% and 9.5% when correlated to normal injection timing. The biodiesel of kapok oil methyl ester is utilized as an alternative fuel in the base engine to obtain better optimum results.

Keywords Injection timing · Retardation · Advanced · Kapok oil methyl ester · Nanoparticles

Abbreviations

SIT KC1 – RET	B20 with cobalt 50 ppm in Retardation
SIT KC2 – RET	B20 with cobalt 100 ppm in Retardation
SIT KC3 – RET	B20 with cobalt 150 ppm in Retardation
SIT KC4 – RET	B20 with cobalt 200 ppm in Retardation
SIT KC1 – ADV	B20 with cobalt 50 ppm in Advanced
SIT KC2 – ADV	B20 with cobalt 100 ppm in Advanced
SIT KC3 – ADV	B20 with cobalt 150 ppm in Advanced
SIT KC4 – ADV	B20 with cobalt 200 ppm in Advanced
CO	Carbon monoxide
BSEC	Brake Specific Fuel Consumption
CO_2	Carbon dioxide
ID	Ignition Delay
BTE	Brake Thermal Efficiency
BSFC	Brake Specific Fuel Consumption
HC	Hydrocarbon
NOx	Oxides of nitrogen
D100	Diesel
A	Algae biodiesel
B5	5% biodiesel + 95% diesel
B10	10% biodiesel + 90% diesel
B20	20% biodiesel+ 80% diesel
B30	30% biodiesel+ 70% diesel
B100	100% biodiesel
C	Camelina sativa and neem seed oil
S	sunflower oil methyl ester
K20	20% Kapok methyl ester+80% diesel

✉ Anbarasan Baluchamy
anbarasan5mech@gmail.com

[1] Department of Mechanical Engineering, PSNA College of Engineering and Technology, Dindigul, Tamil Nadu 624 622, India

Published online: 12 March 2021

1 Introduction

The industrial and transport sectors want an alternative diesel engine fuel considering its availability in the local market and lower emissions. The crude vegetable oil can't be directly utilized in the diesel engine due to its greater viscosity and density [1]. Using raw vegetable oil leads to some problems in the engine i.e., oil deposits in the combustion chamber. To reduce the viscosity and density preheating process is used. The trans-esterification process takes more time to produce biodiesel as compared to the preheating process. The process of preheating takes place at the optimum temperature of 110 °C. Many researchers have prepared various blends of B10, B20, and B30 to B100 etc. [2]. Among the various blends, the B20 blend gives the optimum results when correlated to base fuel (i.e. diesel) [3]. The algae biodiesel is used without any fuel modification in the base engine. The biodiesel algae are mixed in various proportions with the base fuel to prepare A10, A20, A30, A40, and A100 blends. The A20 blend shows lower emission and best performance characteristics correlated to the diesel. The blend A20 shows grater BTE, and TFC is 28% and 10%, respectively, when correlated to the base fuel. It can be attributed due to the less ignition delay and more fuel injected during the combustion process. The algae biodiesel enhances the cylinder pressure by 15% as correlated to the neat base fuel. The hydrocarbon and carbon monoxide are declined by 62% and 38%, respectively, for the blend A30 when correlated to neat base fuel, because of the oxygen availability within the fuel. The opacity of smoke reduced by 30% for the blend A100 when correlated to the neat base fuel because of lesser combustion temperature. The oxide of nitrogen decreased by 39% for the blend A20 when correlated to the base fuel due to improvement in the combustion process [4].

The *Camelina sativa* and neem seed oil are utilized as biodiesel fuel in the base engine. The four different types of fuel blends were prepared by mixing biodiesel with diesel B5, B10, C5, and C10, respectively. The blend C10 gives a better outcome when compared with the remaining tested fuels. The carbon monoxide and hydrocarbon emissions are lowered by 12.09% and 20.37%, respectively, when correlated to the base fuel due to an improvement in the fuel's atomization. The carbon dioxide emission decreased by 6.74% for the blend C10 compared to the base fuel because of the proper air-fuel ratio and rapid combustion process. For the blend C10, the oxides of nitrogen increased by 19.78% relative to the base fuel because of the greater in-cylinder temperature during the combustion process. The blend C10 showed a 3.8% rise in brake thermal efficiency when correlated to the smooth base fuel due to oxygen availability within the fuel [5]. The sunflower oil was blended with the base fuel in this experiment. The S10, S20, and S30 blends are produced utilizing the stirring method. The S20 blend reveals a 7.8% rise in-cylinder pressure when correlated with the base fuel because of the better oxidization of the fuels and elevated temperature through the process of combustion. The S20 blend shows an elevated heat release rate of 5.6% when correlated with the base fuel because of the high temperature produced through the process of combustion [6]. Rapeseed oil was utilized in the base engine. The oil was mixed with the diesel to prepare various blends such as B10 and B20, respectively. The B10 blend exhibits the maximum torque when correlated to other fuel blends. The blend B20 reveals lesser CO and NOx by 12.31% and 9.7%, respectively, when correlated with the neat base fuel. It can be attributed due to shorter ignition timing and the oxygen availability within the fuel. The blend B20 exhibited 6.7% enhancement in brake thermal efficiency when correlated to the neat base fuel because of the greater number and the fuel's oxygen availability. The B20 blend showed a lesser Specific Fuel Consumption of 8.9% when correlated to the neat base fuel [7].

The mixing of nanoparticles in biodiesel exhibits better performance, emission, and combustion characteristics in the engine. It is due to the availability of oxygen in the fuel and nanoparticles, which provide assistance in fuel's rapid combustion. The fish oil was utilized in the experiments and converted to biodiesel using the trans-esterification process. The nanoparticle of 60 ppm graphite oxide was used and mixed with various blends of ethanol and biodiesel. The mixtures were prepared with graphite oxide of 60 ppm, 10% (by volume) biodiesel, and 90% (by volume) diesel, and ethanol was added in different percentages of 2%, 4%, and 6% keeping diesel volume constant. The engine's torque and power increases when nanoparticles are blended with biodiesel as the oxygen becomes accessible inside the fuel. Hydrocarbon and carbon monoxide emissions were lowered by 42.05% and 35.21% for B10 + 6% of bioethanol +60 ppm of graphite oxide when compared to diesel fuel. For blend B10 + 6% of bioethanol +60 ppm, carbon monoxide and nitrogen oxides were increased by 20.09% and 15.23% when correlated to base fuel, because of the insufficient oxygen and peak combustion of temperature through the process of combustion [8].

The Pongamia methyl ester was converted into biodiesel using the trans-esterification process and utilized as a fuel for the engine. The nanoparticle used was aluminum oxide, which was mixed with biodiesel. The nanoparticle was mixed with biodiesel at a different doses of 50 ppm and 100 ppm. The biodiesel blended with 100 ppm dosage of nanoparticles enhanced the brake thermal efficiency by 11.5% when correlated to the neat diesel because of the availability of oxygen in the fuel. The biodiesel blended with 100 ppm dosage of nanoparticle enhanced the cylinder pressure and heat released rate because of the shorter ignition delay and more fuel was injected in the in-let manifold. The hydrocarbon, carbon monoxide, and opacity of smoke emission are lowered by 65%, 54%, and 38%, respectively, for the biodiesel blended with

Table 1 Various Biodiesel used in the conventional engine

Feedstock	Fuel blends	Performance Characteristics		Emission Characteristics				Ref.
		BTE	BSFC	CO_2	CO	NOx	UHC	
Jatropha	B100	↓ (5.12)	↑ (14.46)	-	↓ (23.14)	↓ (4.52)	↓ (18.52)	[16]
Soybean	B5, B20, B50, B85	↑ (7.14)	↓ (17.45)	↑ (4.56)	↑ (38)	↑ (12)	-	[17]
Waste oil	B5, B10	↑ (6.14)	↓ (12.14)	↑ (4.12)	↓ (31)	↓ (15.11)	↑ (31.21)	[18]
Jatropha	B10, B20, B30, B50	↑ (5.54)	↓ (8.98)	↑ (13.14)	↓ (16.16)	↓ (7..46)	(37.54)	[19]
Jatropha	B5, B10, B20, B30	↑ (6.2)	↓ (14.12)	↑ (5.47)	↓ (28.14)	↓ (16.54)	↑ (24.12)	[20]
Waste oil	B25, B50, B75	↑ (4.21)	↓ (7.54)	↑ (17.12)	↑ (20.14)	↑ (13.46)	↑ (11.58)	[21]
Chlorella protothecoides	B20, B50, B100	↑ (7.14)	↓ (14.36)	↑ (8.46)	↓ (19.85)	↑ (2014)	↓ (27.14)	[22]
Chlorella vulgaris	B10, B20	↑ (5.17)	↓ (17.58)	↓ (28.45)	↓ (31.12)	↓ (14.37)	↑ (8.45)	[23]

100 ppm dosage nanoparticle compared to the diesel of the higher evaporation rate and oxygen content within the fuel. The oxides of nitrogen increased for biodiesel blend with 100 ppm dosage of nanoparticle compared to diesel due to peak combustion temperature during the combustion process [9].

Pongamia methyl ester was used in the diesel engine. The nanoparticles of iron oxide were added in different concentrations of 50 ppm and 100 ppm to the biodiesel. The biodiesel was blended with diesel and nanoparticles of 50 ppm and 100 ppm. The blend B20 with iron oxide nanoparticle of 100 ppm shows an increase in brake thermal efficiency of 14.71% compared to the neat diesel fuel. It is due to an increase in surface area and nanoparticles act as oxygen agent leads to better combustion. The increase in-cylinder pressure and heat release rate for blends B20 with iron oxide of 100 ppm causes rapid combustion in the premixed combustion stage. The hydrocarbon, carbon monoxide, and smoke opacity emissions decreased by 24.14%, 58.12%, and 24.18%, respectively, when the blend B20 and 100 ppm iron oxide was used engine instead of diesel. It is due to the shorter ignition delay period, availability of more oxygen content in fuel and fuel burns rapidly during the combustion process. The oxides of nitrogen emission increased of 18.36% for the blend B20 and 100 ppm iron particles as compared to diesel due to the high elevated temperature during the combustion process [10]. The various oils were used in the diesel engine and mixed with diesel in various blends. The two blends, 5% (by volume) of biodiesel and 95% of diesel and 10% of biodiesel and 90% of diesel, were prepared. The nanoparticles were added in various concentrations of 50 ppm and 100 ppm with the biodiesel. The brake thermal efficiency increased by 3.36% for the blend of biodiesel 5%, diesel 95%, and 100 ppm of cerium oxide as compared to the neat diesel because of the increased surface area to volume ratio and shorter ignition delay period. The hydrocarbon, carbon monoxide, and opacity of smoke emission reduced by 4.5%, 13.33%, and 7.46%, respectively, for the blended of biodiesel 5%, diesel 95%, and 100 ppm of cerium oxide when correlated to the base fuel due to the presence of nanoparticles in the fuel. The oxides of nitrogen emission for the blended of biodiesel 5%, diesel 95%, and 100 ppm of cerium oxide increased as compared to the base

Table 2 The Various nanoparticles mixed with biodiesel used in the conventional engine

Nanoparticle additive	Performance Characteristics		Emission Characteristics			Combustion Characteristics		Ref
	BTE	SFC	CO	NOx	UHC	HRR	PP	
Alumina Al_2O_3	↑ (5.38)	↓ (11.46)	↑ (58.12)	↑ (9.8)	↑ (42.8)	↑ (20)	↑ (2.5)	[24]
AL, Fe, Bo nano particles	↑ (9.12)	↓ (7)	↓ (40.14)	↓ (8)	↑ (12)	↓ (11.41)	↓ (11.29)	[25]
Cerium oxide	↑ (6.5)	↓ (9.1)	↓ (37)	↓ (30.12)	↓ (40.54)	↓ (8.14)	--	[26]
$Fecl_3$ powder	↑ (3.1)	↓ (18.4)	↓ (52.6)	↑ (6.5)	↓ (1.8)	↑ (4.6)	↑ (4.2)	[27]
Silver	-	-	↑ (54)	↓ (36)	↑ (28)	↓ (24.12)	↓ (12.4)	[28]
Nano organic additive Glycerin	↑ (12)	-	↑ (34)	↓ (30)	↑ (68)	↓ (3.2)	↓ (4.65)	[29]
CNT	↑ (14.7)	↓ (13)	↓ (29)	↓ (6.4)	↑ (15.25)	↑ (10.21)	↑ (15.68)	[30]
CNT	↑ (6.38)	↓ (27)	↓ (41.21)	↑ (65)	↓ (26.14)	↑ (16.54)	↓ (33.11)	[31]
Ceo_2	↓ (5.21)	↓ (12.14)	↓ (38.54)	↓ (21.54)	-	↑ (5.68)	↑ (6.12)	[32]

Table 3 Various biodiesel used in the injection timing

Injection Timing	FUEL USED	Performance		Emission Characteristics				Ref
Degree °C		BTE	BSEC	HC	CO	NOx	Smoke	
22	Isobutanol/diesel	↑ (2.5)	↓ (8.4)	↑ (14.4)	↓ (24.4)	↑ (18.4)	↓ (14.1)	[33]
23	Isobutanol/diesel	↑ (4.2)	↑ (12.4)	↑ (17.2)	↓ (21.7)	↓ (13.4)	↓ (15.5)	[33]
23	n- Pentanol/diesel	↑ (5.1)	↑ (11.4)	↑ (15.2)	↓ (18.5)	↑ (12.25)	↓ (14.5)	[33]
21	Waste Plastic oil	↓ (1.8)	↑ (4.6)	↑ (12.4)	↓ (12.2)	↓ (13.6)	↑ (14.1)	[34]
23	Waste Plastic oil	↑ (4.5)	↑ (6.1)	↑ (10.4)	↓ (20.1)	↑ (13.4)	↓ (13.7)	[34]
25	Waste Plastic oil	↑ (8.7)	↑ (12.4)	↑ (11.4)	↓ (21.4)	↑ (10.4)	↓ (14.3)	[34]
19	D94W5S1 – SI25	↓ (2.4)	↑ (7.1)	↑ (8.9)	↓ (13.5)	↓ (5.6)	↓ (10.2)	[35]
21	D94W5S1 – SI50	↓ (1.2)	↑ (10.5)	↑ (9.5)	↓ (14.2)	↓ (12.9)	↑ (9.5)	[35]
23	D94W5S1 – SI75	↑ (4.6)	↑ (11.2)	↑ (12.3)	↓ (15.3)	↓ (14.5)	↓ (13.2)	[35]
19	Algae – BHT	↓ (3.3)	↑ (8.4)	↑ (8.4)	↓ (12.6)	↓ (6.2)	↓ (9.2)	[36]
21	Algae – BHT	↓ (2.1)	↑ (10.2)	↑ (10.2)	↓ (14.56)	↓ (8.5)	↓ (14.5)	[36]
23	Algae – BHT	↑ (6.2)	↑ (13.2)	↑ (11.2)	↓ (21.1)	↓ (11.6)	↓ (17.6)	[36]

fuel, because of the elevated cylinder temperature produced during the combustion process [11].

Many researchers have suggested introducing the injection timing (IT) parameter into the biodiesel with nanoparticles to give the optimum results. When using, the oxides of nitrogen increased for the blend of biodiesel with nanoparticles. The injection timing parameter was introduced to overcome this problem [12]. The pyrolysis oil was combined with plastic oil and used in the engine. The various biodiesel blends B10, B20, and B30 are prepared. The brake thermal efficiency for blend B20 was 14.56% higher as compared with the base fuel, because of the advanced IT, shorter ignition delay, and availability of oxygen in the fuel. The hydrocarbon (HC), carbon monoxide (CO), and opacity of smoke emission in the blend B20 are decreased by 21.12%, 18.87%, and 22.45%, respectively, when correlated with the base fuel because the proper combustion of the fuel takes place. The HC, CO, and opacity of smoke emission increase when the IT was retarded. The nitrogen oxides (NOx) emission increased by 12.56% for blend B20 when correlated with base fuel because of the elevated temperature during the combustion process [13].

The tamarind seed was utilized as an alternative fuel for the diesel engine. Various blends were prepared and IT was varied to 21 CAD bTDC, 23 CAD bTDC, and 27 CAD bTDC. The IT was advanced and the brake thermal efficiency for the tested fuel B20 increased by 3.78% when correlated to the base fuel because of the shorter ignition delay period. When IT was advanced the heat release rate and in-cylinder pressure were also increased when compared to diesel because of the greater temperature and more fuel burns during the process of combustion. When injection timing was retarded, the HC, CO, NOx, and opacity of smoke emission for the blend B20 were decreased by 11.76%, 10.53%, 32.34%, and 25.47% as compared to diesel [14].

The petroleum-based diesel fuel was combined with diesel and used in the experiments. The tested fuel blends B10, B20, B30, and B40 were prepared and injection timing was varied. The brake thermal efficiency was higher by 3.17% for blend B20 when correlated with the base engine, because of the shorter ignition delay period and more fuel injected in the inlet manifold. The HC, CO, and opacity of smoke emission are decreased when correlated with the base fuel due to the availability of more oxygen in the fuel and shorter ignition delay

Table 4 Composition of Kapok Oil

Name of the Acid	Percentages
Myristic Acid	0.25%
Palmitic Acid	24.31%
Palmitoleic Acid	0.40%
Steraric Acid	2.65%
Oleic Acid	21.83%
Linoleic Acid	38.92%
Arachidic Acid	1.00%
Malvalic Acid	7.18%
Behenenic Acid	0.44%
Sterculic Acid	2.96%

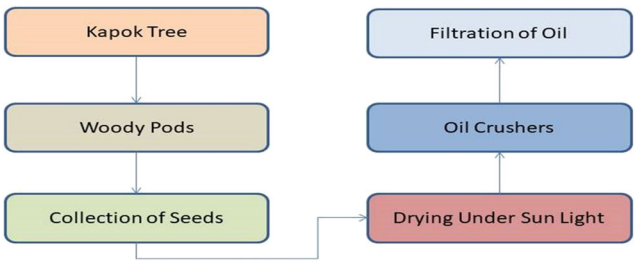

Fig. 1 Extraction Process for Kapok oil

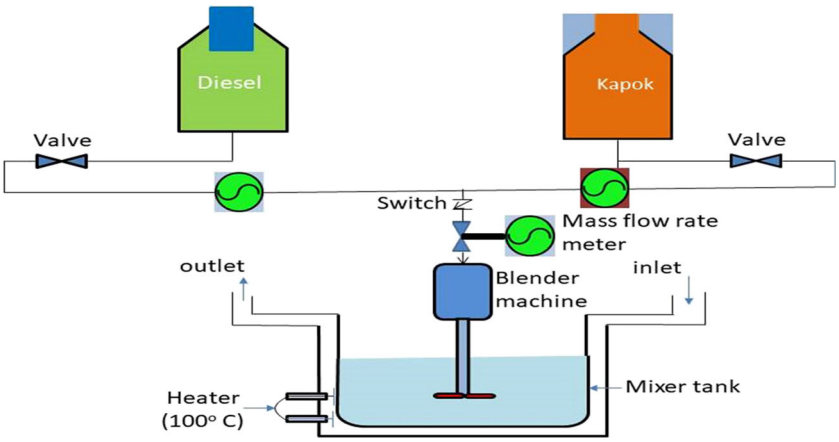

Fig. 2 Preheating Process

period. When IT was advanced, the NOx emission increased by 8.32% when correlated with the base fuel due to the elevated temperature during the combustion process [15].

From the detailed literature survey, it was found that the biodiesel blend B20 showed superior performance, emission, and combustion characteristics than the other blends. This is due to the shorter ignition delay period and complete combustion of the fuel. The addition of nanoparticles with biodiesel resulted in better engine characteristics. The main motivations of the present research are discussed further. (i) Diesel-powered conventional compression ignition (CI) engine produced high NOx and smoke emission. Many researchers reported that biodiesel operated CI engine emits lesser smoke emission but shows high NOx emission. (ii) The partial or full replacement of diesel fuel with biodiesel can achieve reasonable power and emits low HC and CO emissions but high NOx emission. (iii) The utilization of biodiesel and nanoparticles in the engine produced more NOx emission because of the higher in-cylinder temperature which resulted in a better combustion process. (iv) To overcome the formation of NOx, injection strategies were utilized to reduce the NO_X emission reasonably. (v) The combined effect of nanoparticle and varying the injection timing leads to produce significant improvement in performance and reduction in emission characteristics. The ultimate objective of the present research is to investigate effective use of kapok biodiesel as a fuel in CI engine. Subsequently, assess the impact of nanoparticles addition with kapok biodiesel on the engine. Finally, analyze the engine characteristics by varying the injection timing at a constant speed.

Various biodiesel was used in the conventional engine as shown in Table 1. Two symbols have been used in the table, one is upward and another is downward. The upwards symbol shows the increase and downward symbol shows the decrease in the parameters.

Table 2 shows the various nanoparticles mixed with biodiesel used in the conventional engine. Two symbols have been used in the table, one is upward and another is downward. The upwards symbol shows the increase and downward symbol shows the decrease in the parameters.

Table 3 Various biodiesel is used in the injection timing. Two symbols have been used in the table, one is upward and another is downward. The upwards symbol shows the increase and downward symbol shows the decrease in the parameters.

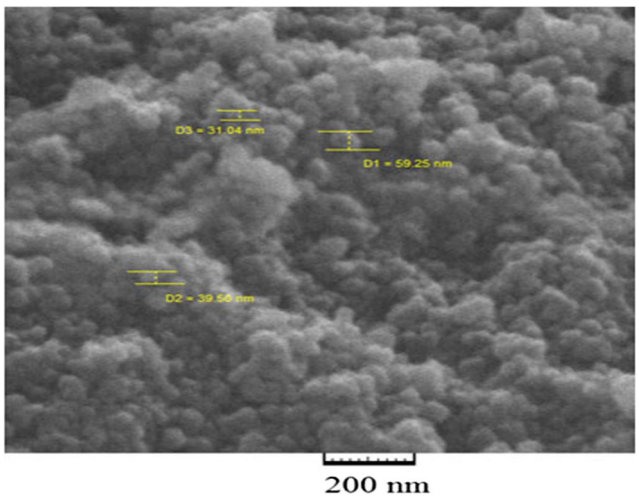

Fig. 3 Cobalt Chromite for SEM image

Table 5 Cobalt Chromite property

Color	Blue
Chemical Name	Cobalt Chromite Blue-Green Spinel
Chemical Formula	$Co(Al, Cr)_2O_4$
Particle Size	1.0 μm
Density	4.7 g/cm^3
Refractive Index	1.560–1.662
Oil Absorption	5 g oil / 100 g pigment

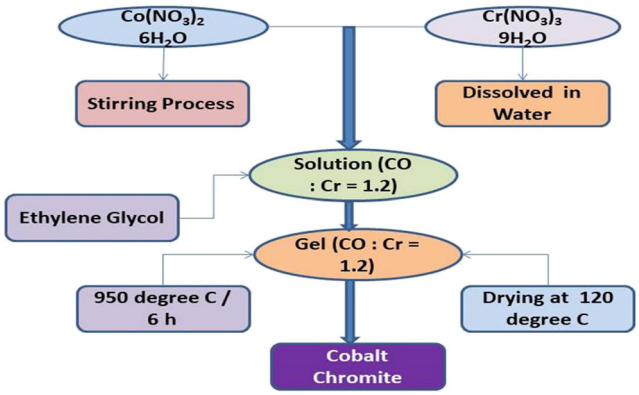

Fig. 4 Preparation of Cobalt Chromite

2 Materials and methods

2.1 Overview of kapok oil

The oil is yellowish in color with a lovely scent smell like consumable oil. Kapok oil is not suitable for consumption because of the quality of cyclopropenoid greasy acids [37]. It contains 39 unsaturated fats that can be utilized as a fuel for the base engine in the form of kapok oil methyl ester (KOME). Table 4 shows the composition of kapok oil.

2.2 Extraction process of oil

Kapok Woody units were gathered in Tamilnadu, India. The seeds of kapok are isolated from the silky fiber in the woody cases [38]. These seeds were dried under the daylight until their shading changed and taken care in an enormous extractor limit compartment. The extraction of oil from Kapok seed was accomplished using a mechanical crusher. The raw crude kapok oil was collected and filtered to eliminate the contaminations. Figure 1 shows the flow diagram of the Kapok seed oil extraction process.

2.3 Preheating process

The crude vegetable oil cannot directly have utilized in the engine. Thus, viscosity and density of the fuel were lowered using the preheating process. The trans-esterification process is the oldest method; nowadays, many researchers have suggested the preheating method [38]. In the preheating process, biodiesel is produced with less time as compared to the trans-esterification process. The preheating process can be done by two methods, one is heat exchanging and another is by a heater. The preheating temperature was maintained between 60 °C to 120 °C and the optimum result was achieved at 110 °C. Figure 2 shows the preheating process of the oil.

2.4 Nanoparticles of cobalt chromite

Figure 3 shows the SEM image of cobalt chromite. An ordinary co-precipitation strategy was utilized to incorporate cobalt chromite nanoparticles. Arrangement of cobalt nitrate (0.5 μm), chromium nitrate (1 μm), and smelling salts arrangement (25%) were set up in 25 ml volumetric jars independently by dissolving suitable measure of them in refined water, separately. The required amount of cobalt nitrate arrangement was taken in a 100 ml measuring glass, and afterward, chromium nitrate arrangement was included gradually to it under persistent blending. The blended arrangement was mixed at room temperature for 2 h. At a particular point, fluid smelling salt arrangement (25%) is included in a dropwise manner to the blended arrangement till the pH of 9. The hydroxide accelerate was shifted and washed for few times with refined water till the filtrate accomplishes a pH of around 7 [39]. The acquired hasten was dried on

Fig. 5 Fuel preparation for the oil

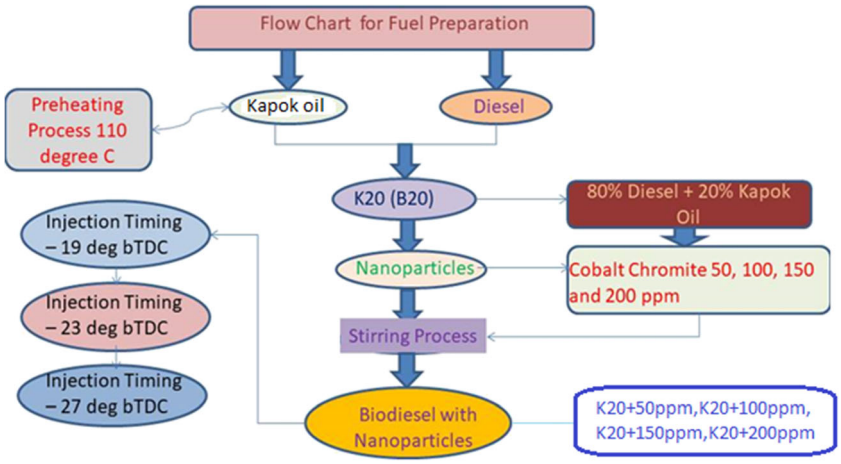

Table 6 Fuel Properties of the fuel

Property	Diesel	Raw Oil	B20+50 ppm	B20+50 ppm	B20+50 ppm	B20+50 ppm
Specific gravity(40 °C) (kg/m^3)	0.85	0.875	0.861	0.856	0.857	0.849
Density (40 °C) (kg/m^3)	822	931	845	856	875	867
Viscosity(40 °C) mm^2 /S	3.1	4.2	3.8	3.7	3.9	3.4
Calorific Value MJ/m^3	44	38	39	38	40	42
Cetane Number	54	48	49	51	52	56
Acid Number	–	0.2	0.5	0.4	0.6	0.2
Fire Point (^{0} C)	74	174	154	162	165	161
FlashPoint(^{0} C)	59	170	145	151	159	165

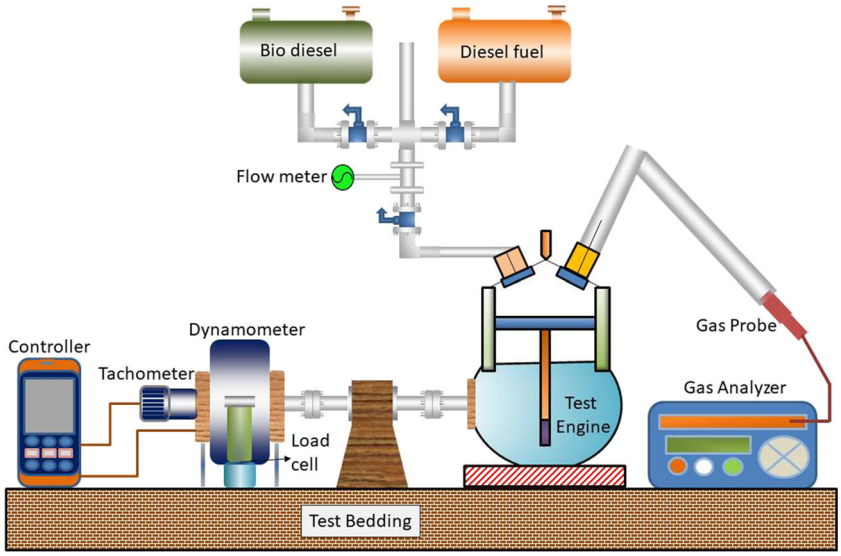

Fig. 6 Experimental Setup

a stove at 120 °C for 16 h and calcined at 600 °C for 4 h to get well jasper green powder. The nanoparticles of cobalt chromite was chosen in the present study because of its higher oxygen content as compared to the other nanoparticles. Table 5 shows the property of cobalt chromite. Figure 4 shows the preparation of cobalt chromite.

Table 7 Specifications of the Engine

Specification of Engine	
Brand and Model	Kirloskar, SV1
Number of cylinders	1
Cooling Types	Water-cooled
Stroke volume	661 cc
Engine speed	1800 rpm
No. of strokes	4
Clearance volume	37.8
Rated output	5.9 kW
Diameter of Bore	87.5 mm
Length of Stroke	110 mm
Lubrication system	Forced feed system
Compression Ratio	17.5:1

Table 8 Uncertainty Analysis

S. No.	Parameters	Systematic Errors (%)
1	Speed, rpm	1
2	Load, N	0.2
3	Time, seconds	0.1
4	Brake Power, kW	0.5
5	Temperature, ^{o} C	1
6	Pressure, bar	1
7	NO_x, ppm	9
8	CO, %	0.03
9	CO_2, %	0.03
10	Unburnt hydrocarbon, ppm	10
11	Smoke, HSU	1

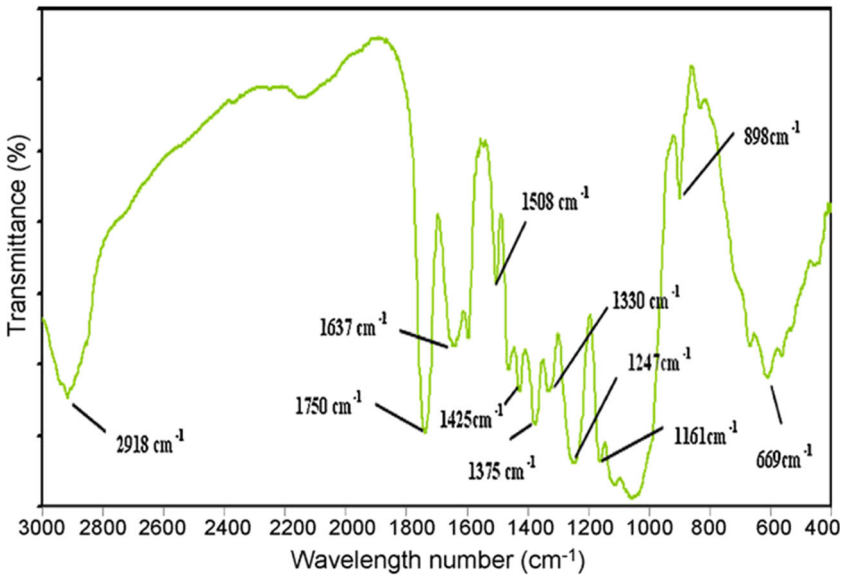

Fig. 7 FTIR Analysis for Kapok Oil

2.5 Fuel preparation

The preheated Kapok oil was utilized in the base engine with no significant adjustments. The oil was heated up to 110 °C with the help of the preheating process to decrease the density and viscosity of the fuel. The kapok biodiesel was blended with the base fuel and various blends are prepared [40]. The nanoparticles were mixed with the kapok biodiesel using mechanical stirring. The B20 blend was mixed with the nanoparticles at various dosages of 50 ppm, 100 ppm, 150 ppm, and 200 ppm. The different blends were prepared by varying the injection timing, such as 19 CAD bTDC, 23 CAD bTDC, and 27 CAD bTDC. These results were correlated to standard injection timing. Figure 5 shows the fuel preparation from the oil. Table 6 indicates the properties of the fuel.

3 Experimental set-up

The single-cylinder four-strokes direct-injection conventional engine was utilized for the experimental purpose and Fig. 6 shows the base engine set-up. The specification of the base engine is shown in Table 7. After inspection, instruments were arranged, the exhaust emission parameters were calibrated. The base engine was coupled with the eddy current dynamometer. The base engine speed was maintained at 1500 rpm and 5.1 kW of rated power. The AVL 444 N gas analyzer was utilized to quantify the emission parameters like CO, CO_2, NOx, and hydrocarbon. The power of the smoke meter is estimated with the assistance of the AVL 443 N smoke meter. The IT was varied by impeding and propelling the position when contrasted and the standard IT. The RIT (19 CAD bTDC), SIT (23 CAD bTDC), and AIT (27 CAD bTDC) were used in this investigation.

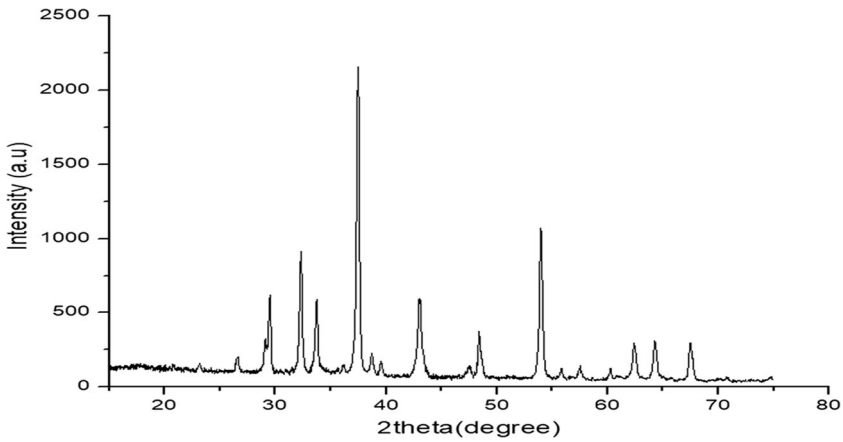

Fig. 8 XRD Analysis for Kapok Oil

3.1 Uncertainty analysis

Uncertainty analysis was used to calculate the range of errors. The reading of the diesel engine varies slightly with the instruments' condition and vibration. To reduce these types of errors in the diesel engine, uncertainty analysis is adopted. The engine was started and operated for up to half an hour, and reading was taken from the diesel engine [41]. Five times with the same blend readings were recorded, and the average values were used to plot the graph. The range between the measured value plus or minus to systematic error gives the uncertainty values. Table 8 shows the uncertainty analysis.

3.2 FTIR analysis

The sample is loaded in the FT-IR spectroscopy, and a relevant peak for Kapok oil was generated and the result is plotted in Fig. 7. The Kapok oil has some feeble peaks from 1700 to 3000 cm^{-1}, which is consistent of C-H band. FT-IR results in the N-H band at 1236 cm^{-1} that support the presence of biomolecules besides cobalt chromite. Then, the sharp peak 3492 cm^{-1} reveals the N-H band's existence in the sample, and it is broader than the other generated peak in this region, namely, aromatic ring and carbonyl stretching modes. At 1746 $cm^{-1.}$ a scissoring in-plane twisting approach of NH_2 amine group is available.

3.3 XRD analysis

Figure 8 displays the XRD analysis of Kapok oil. The deflection peaks at 2θ of 40, 46, and 66 related to (1 1 1), (2 0 0), and (2 2 0) were associated with the planes. The deflection peak (1 1 1) mean particle size is inveterate by Scherrer's method. The inveterate mean particle size is about 5.2 nm. Finally, the result accepts the presence of kapok oil in the sample with a corresponding nanometer size and boosts the reaction's catalytic activity.

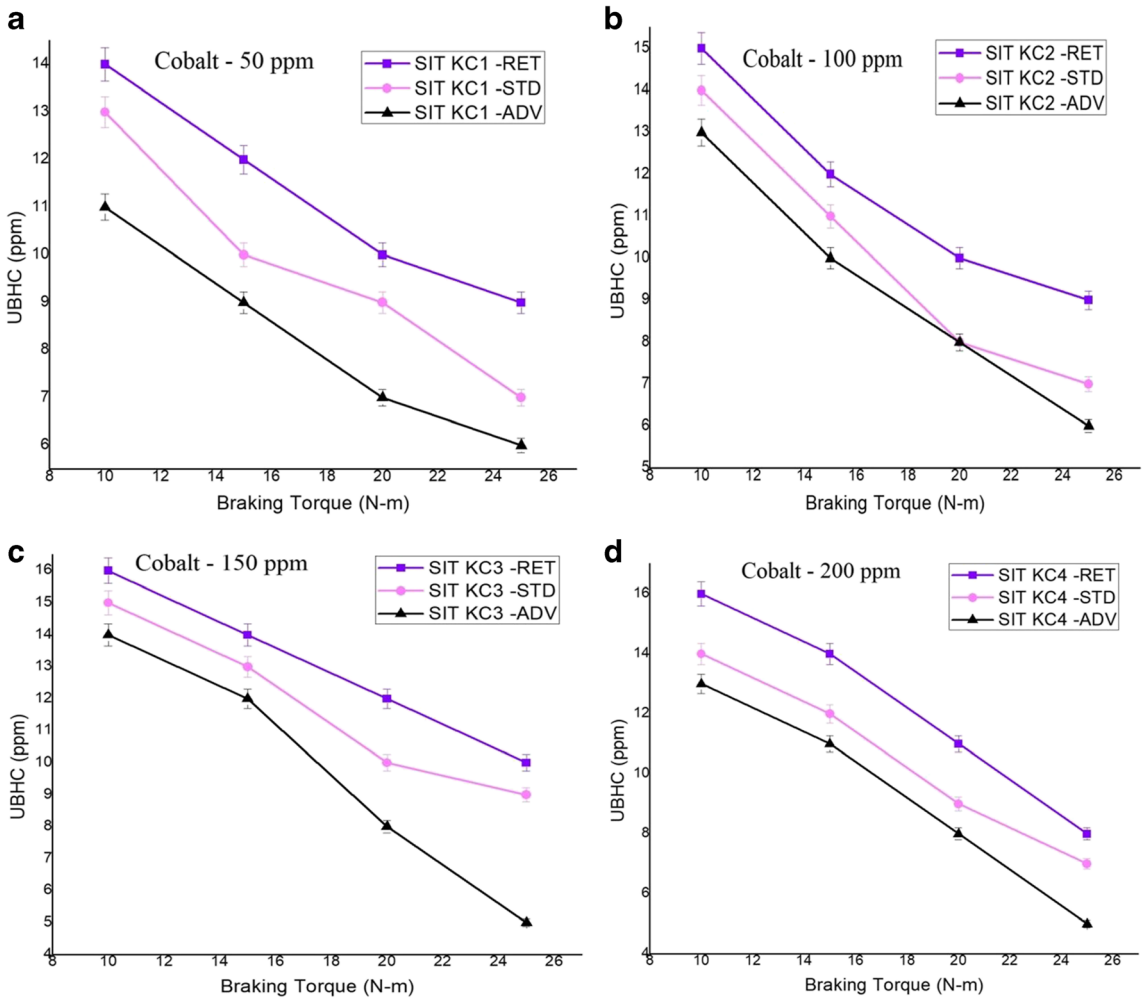

Fig. 9 Variation of braking torque Vs UBHC

4 Result and discussion

4.1 UBHC

Figure 9 shows the variations of hydrocarbon and brake torque of various fuel blends, i.e., K20 and 50 ppm, K20 and 100 ppm, K20, and 150 ppm, and K20 and 200 ppm for different injection timing. At retardation of fuel injection timing deposited into the cylinder walls was high, and at lower fuel injection timing, the fuel spray penetration on the surface piston is high [42]. The presence of cobalt chromite nanoparticles to reduce the hydrocarbon emission in the combustion process due to the presence of nanofluid. When IT was advanced (27 CAD bTDC), there was a drastic reduction of unburnt hydrocarbon at all load conditions. The presence of nanoparticles within the fuel is responsible for proper combustion. The nanoparticles in the tested fuel K20 led to higher surface tension, which resulted in lesser compressibility and greater viscosity of the fuel. The nanoparticles led to a greater surface area to volume ratio, which improved the fuel's combustion, thereby lowered the hydrocarbon as correlated with diesel [43]. When IT was retarded, the hydrocarbon emission increased. When the IT was advanced the hydrocarbon emission for the blends SIT KC1 -ADV, SIT KC2 -ADV, SIT KC3 -ADV, and SIT KC4 -ADV decreased by 31.33%, 33.32%, 35.72%, and 37.68% when compared with the 23 CAD bTDC (i.e., standard injection timing) due to the oxidation reaction and shorter ignition delay.

4.2 CO

Figure 10 shows the variations of CO and brake torque of various fuel blends, i.e., K20 and 50 ppm, K20 and 100 ppm, K20, and 150 ppm, and K20 and 200 ppm for different injection timing. When IT was advanced, it resulted in a drastic decrement in carbon monoxide and a higher

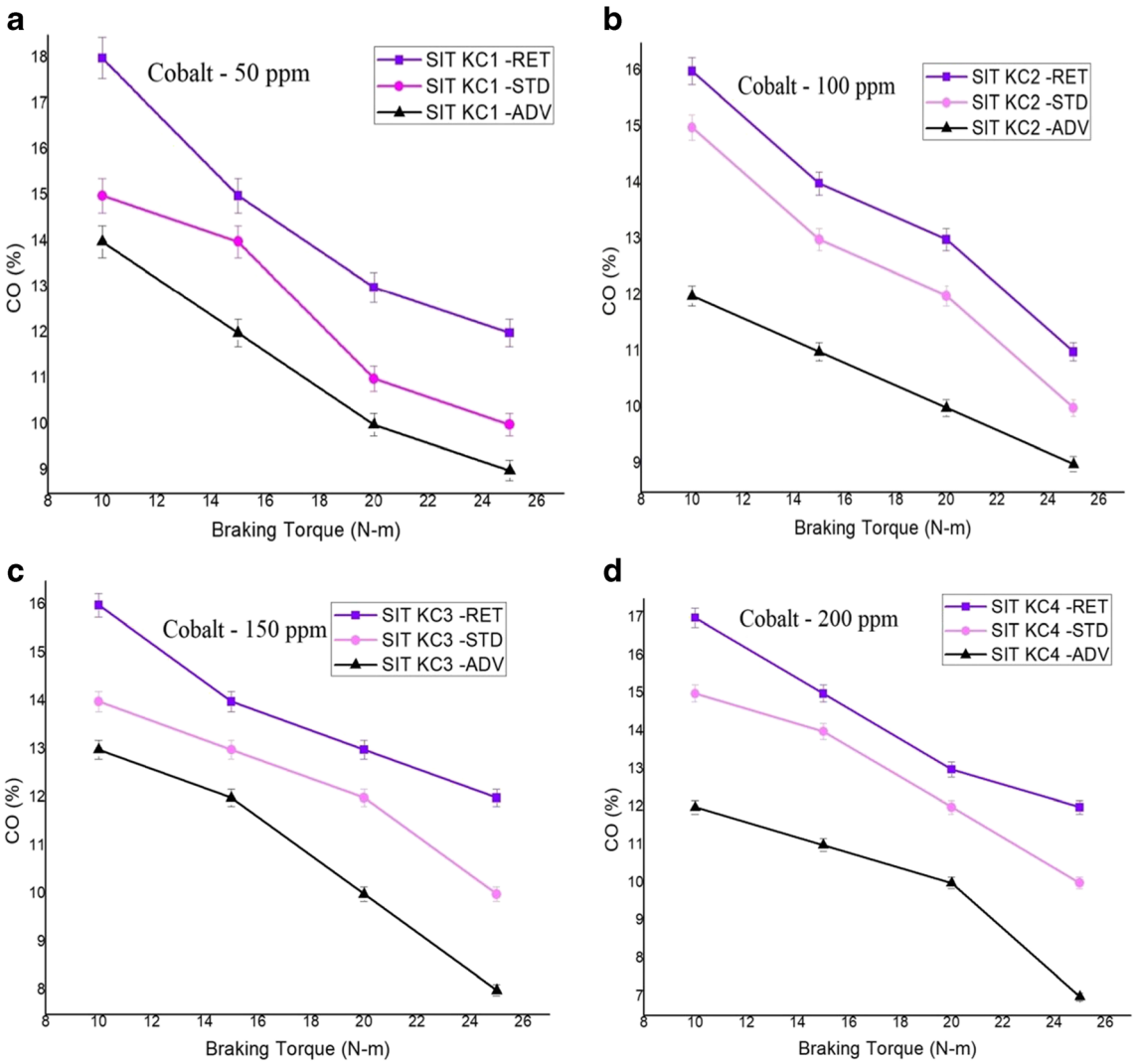

Fig. 10 Variation of braking torque Vs CO

carbon monoxide when fuel injection timing is retarded. Many researchers had proved that CO can be decreased when biodiesel was used as a fuel in the base engine because of the availability of oxygen in the fuel and shorter ID period. The methyl esters have adopted a sub-atomic structure of oxygen ions. When IT was advanced, it resulted in higher in-cylinder pressure, temperature by the oxidation process between the oxygen and the carbon atoms, thereby increasing the ignition delay [44]. When the IT was advanced, carbon monoxide emission for the blends SIT KC1 -ADV, SIT KC2 -ADV, SIT KC3 – ADV, and SIT KC4 -ADV decreased by 25%, 29.12%, 33.33%, and 41.66%, respectively, when correlated to the 23 CAD bTDC (i.e., standard injection timing). Adding the nanoparticles at lower load conditions into the fuel has not decreased CO emissions, whereas at higher load conditions, there was a significant reduction in carbon monoxide. It is due to the nanoparticle that acted as an oxygen buffer and provided sufficient oxygen for complete combustion of the fuel.

4.3 CO_2

Figure 11 illustrates the variations of CO_2 and brake torque of various fuel blends, i.e., K20 and 50 ppm, K20 and 100 ppm, K20, and 150 ppm, and K20 and 200 ppm for different injection timings. When the IT was advanced, there was higher carbon dioxide emission, and when the IT was retarded there was a decrement in carbon dioxide emission. At the SIT, the carbon dioxide was higher, because of oxygen availability within the fuel. The carbon dioxide decreased for all load conditions when the IT was retarded to 19 CAD bTDC. When the injection timing was retarded the carbon dioxide emission for the blends SIT KC1 - RET, SIT KC2 - RET,

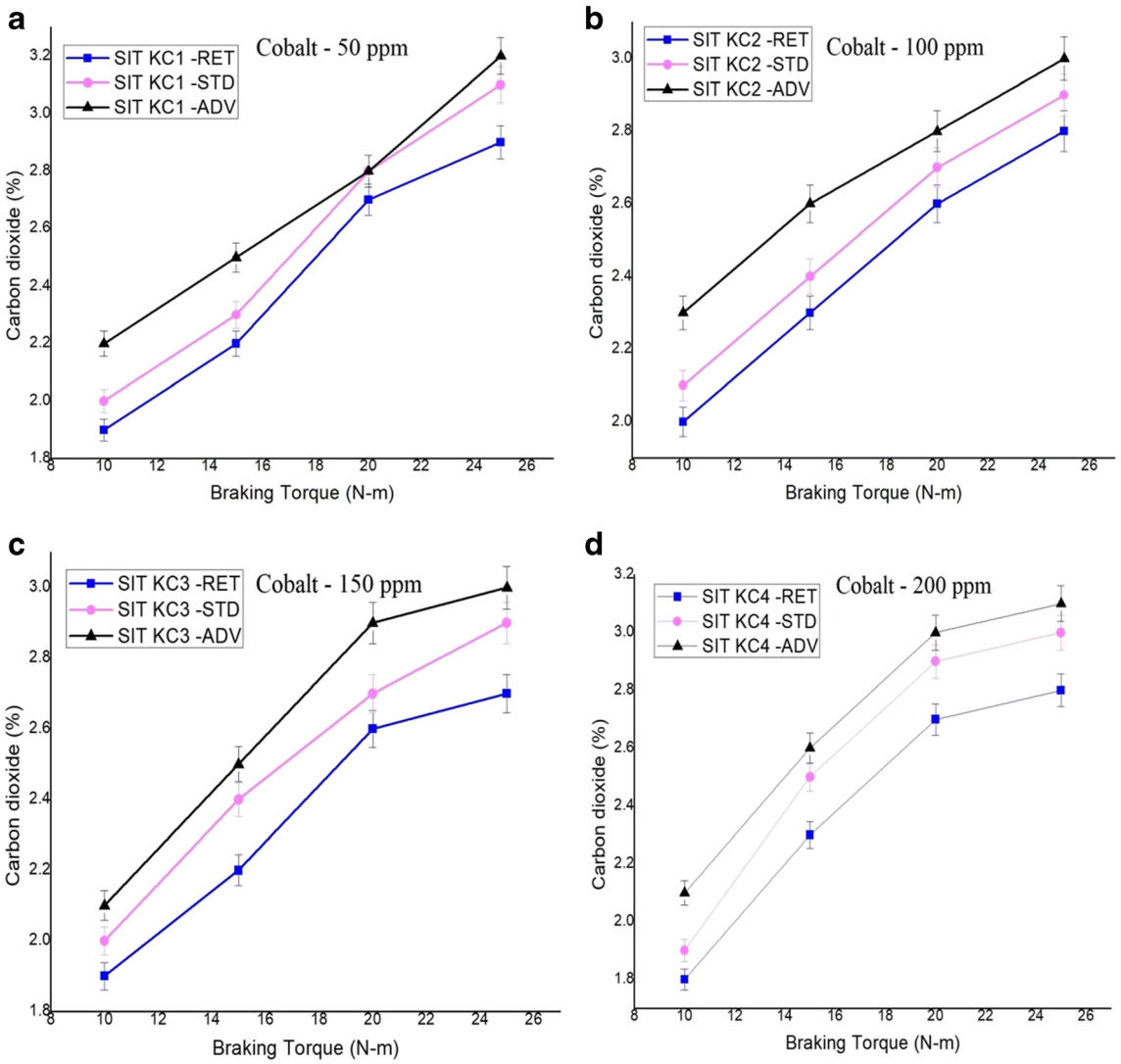

Fig. 11 Variation of braking torque Vs CO_2

SIT KC3 - RET, and SIT KC4 - RET decreased by 6.45%, 3.4%, 7.2%, and 9.5%, respectively, when compared to the 23 CAD bTDC (i.e., standard injection timing) due to better oxidation of fuel in the process of premixed combustion and resulted in shorter ID period. The biodiesel with 50 ppm and 100 ppm dosage of nanoparticles at 23 CAD bTDC and 27 CAD bTDC produced similar results. At 23 CAD bTDC, biodiesel with 150 ppm, 200 ppm dosage of nanoparticles provided slightly higher carbon monoxide emission than advanced injection timing.

4.4 NO_X

Figure 12 shows the variations of carbon monoxide and braking torque of various fuel blends, i.e., K20 and 50 ppm, K20 and 100 ppm, K20, and 150 ppm, and K20 and 200 ppm for different injection timings. The formations of oxides of nitrogen happen at high in-cylinder temperature during the process of combustion. During the retarded position, some reduction of oxide of nitrogen was obtained. It was also found that the oxides of nitrogen decreased when there is an increase in engine load due to a shorter ID period, lesser combustion pressure, and lesser duration of combustion [45]. When nanoparticles were added into the fuel during retarded position, there was no formation of oxides of nitrogen. When IT was retarded, the oxides of nitrogen emission for the blends SIT KC1 - RET, SIT KC2 - RET, SIT KC3 - RET, and SIT KC4 - RET decreased by 9.34%, 12.12%, 14.21%, and 16.45%, respectively, when compared with the 23 CAD bTDC (Standard injection timing) due to shorter ID period and lower temperature

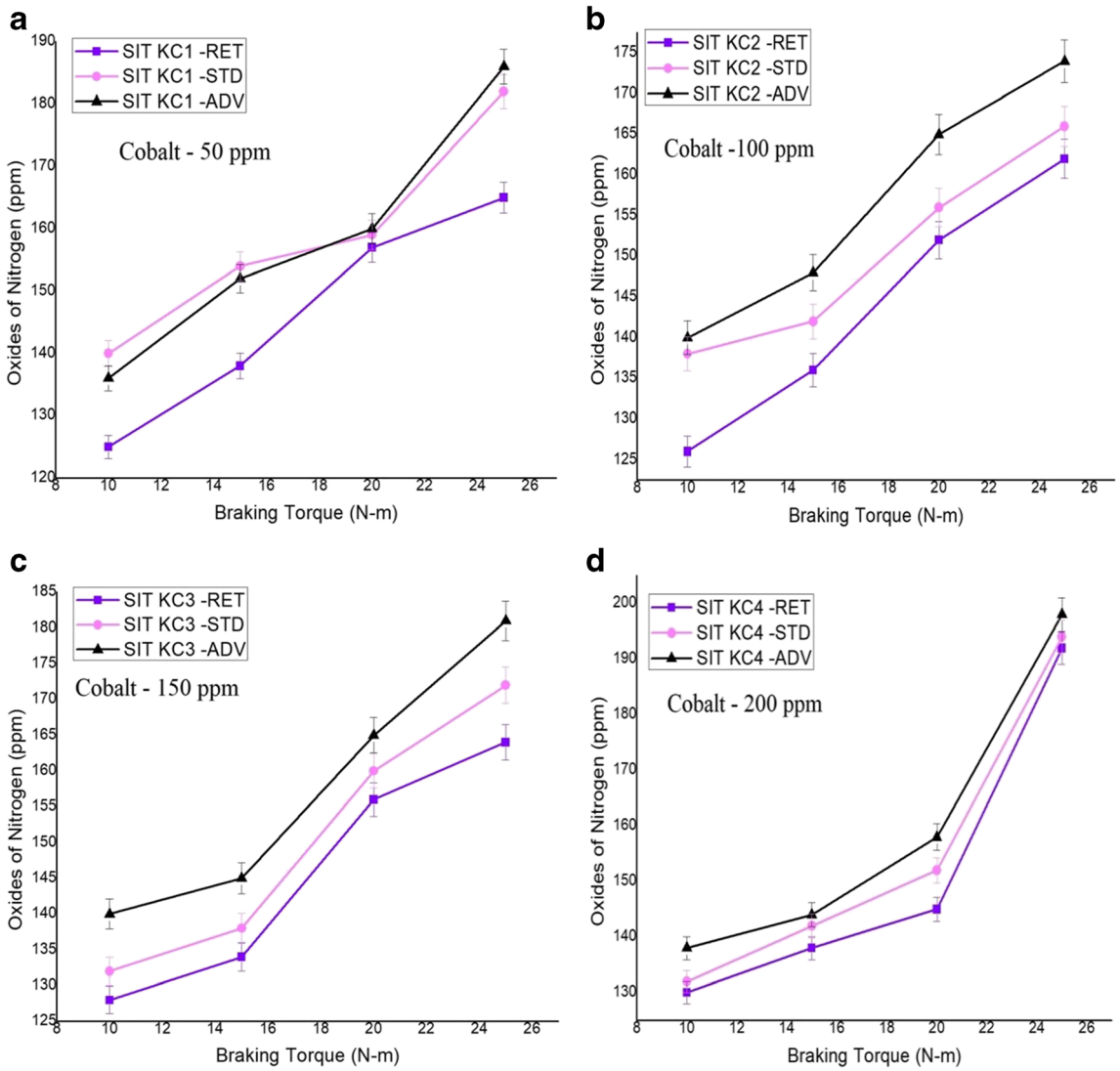

Fig. 12 Variation of braking torque Vs NOx

prevailing through the process of combustion. When AIT, there was an increase in the oxides of nitrogen emission when correlated to the SIT.

4.5 BTE

Figure 13 shows the variations of carbon monoxide and brake torque of various fuel blends, i.e., K20 and 50 ppm, K20 and 100 ppm, K20, and 150 ppm, and K20 and 200 ppm for different injection timings. When IT was advanced, the brake thermal efficiency increased, whereas when IT was retarded the brake thermal efficiency decreased. The 27 CAD bTDC shows the highest brake thermal efficiency due to additional time consumption through the process of combustion. Similar studies showed that the depreciation in brake thermal efficiency for various fuel blends with various injection timings. When IT was retarded, more depreciation was observed as compared to advance IT. The methyl esters have an elevated ignition temperature and higher molecular weight due to late combustion during combustion, which resulted in greater brake thermal efficiency [46]. When the IT was advanced, the brake thermal efficiency for the blends SIT KC1 -ADV, SIT KC2 -ADV, SIT KC3 -ADV, and SIT KC4 -ADV increased by 3.2%, 3.7%, 4.5%, and 7.2%, respectively, when compared with the 23 CAD bTDC (i.e., standard injection timing) due to the presence of nanoparticles in the fuel and fuel burns completely during the combustion process.

4.6 BSFC

Figure 14 illustrates the variations of brake specific fuel consumption (BSFC) and brake torque of various fuel blends, i.e., K20 and 50 ppm, K20 and 100 ppm, K20, and 150 ppm, and K20 and 200 ppm for different injection timings. When fuel IT advanced, the maximum BSFC was attained when correlated to the retarded IT. It is due to the effect of turbulence in the later phase of the combustion process. When the IT was advanced, the BSFC for the blends SIT KC1 -ADV, SIT KC2 -ADV, SIT KC3 -ADV, and SIT KC4 -ADV decreased by 11.76%, 15.45%, 16.76%, and 21.23%, respectively, when compared with the 23

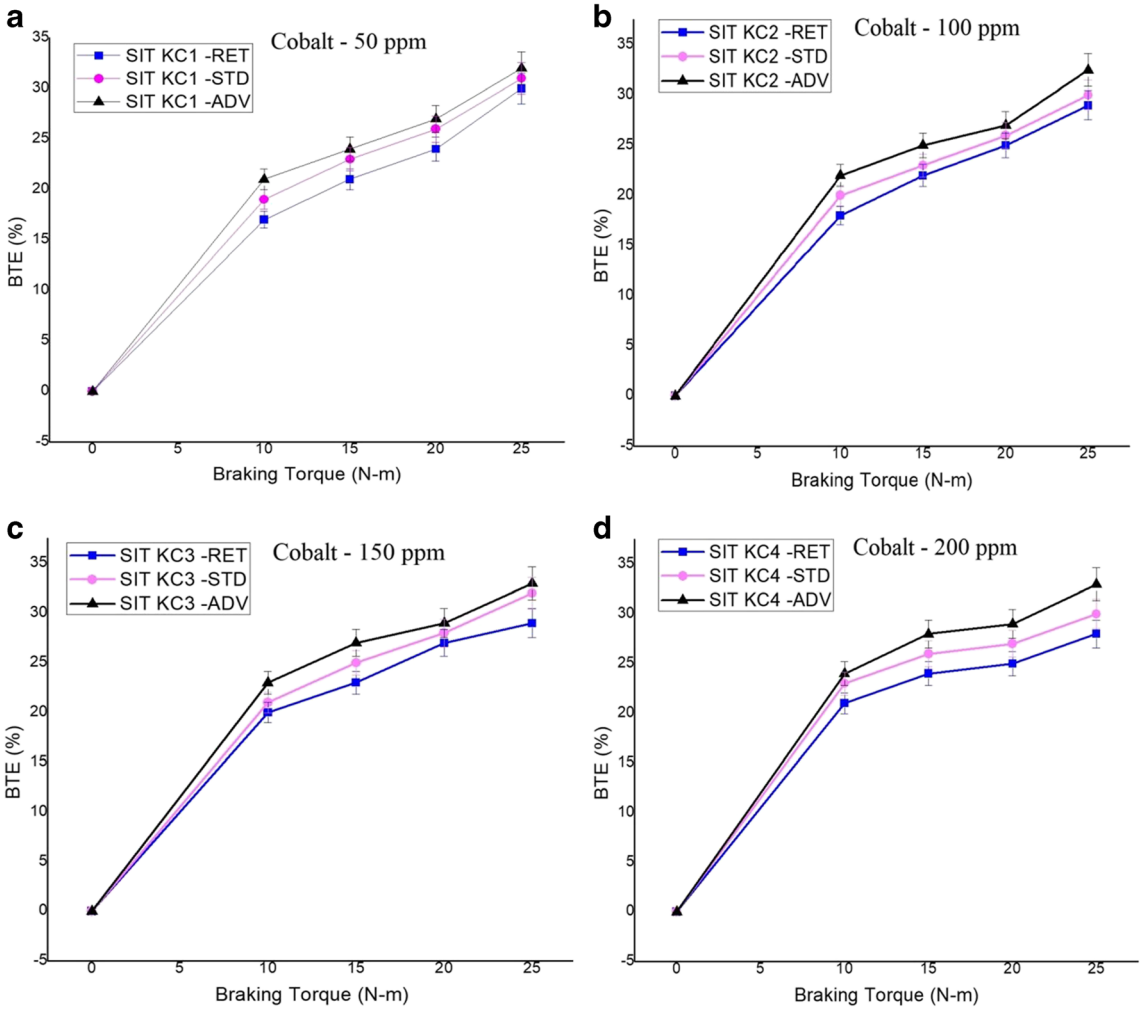

Fig. 13 Variation of braking torque Vs BTE

CAD bTDC (i.e., standard injection timing). It is due to the availability of nanoparticles within the fuel and shorter ID period. The nanoparticle concentration increased the BSFC in both advance and retardation injection timing conditions [47].

4.7 In-cylinder pressure

Figure 15 illustrates the deviations of in-cylinder pressure and braking torque of various fuel blends, i.e., K20 and 50 ppm, K20 and 100 ppm, K20, and 150 ppm, and K20 and 200 ppm for different injection timings. When the IT was advanced, the in-cylinder pressure increased due to the elevated in-cylinder temperature. When the IT was advanced, the in-cylinder pressure for the blends SIT KC1 -ADV, SIT KC2 -ADV, SIT KC3 -ADV, and SIT KC4 –ADV increased by 5.12%, 3.12%, 5.24%, and 5.72%, respectively when correlated to the 23 CAD bTDC (i.e., standard injection timing). It is due to the oxidization reaction within the fuel and complete combustion of fuel during the combustion process [48]. The cobalt nanoparticle mixed with the biodiesel increased the in-cylinder pressure when the dosage of nanoparticles was higher in the blend.

4.8 HRR

Figure 16 illustrates the variation of HRR with braking torque of various fuel blends, i.e., K20 and 50 ppm, K20 and 100 ppm, K20 and 150 ppm, and K20 and 200 ppm for different injection timings. Generally, the HRR increased with an increase in the dosage of nanoparticles due to the higher in-cylinder pressure [49]. When the injection timing was advanced, the HRR for the tested fuels SIT KC1 -ADV, SIT KC2 -ADV, SIT KC3 -ADV, and SIT KC4 –ADV increased by 3.2%, 4.54%, 4.12%, and 5.09%, respectively, when compared with the 23 CAD bTDC (i.e., standard injection timing) because of the availability of the nanoparticles within the fuel and resulted in completely combustion of the fuel.

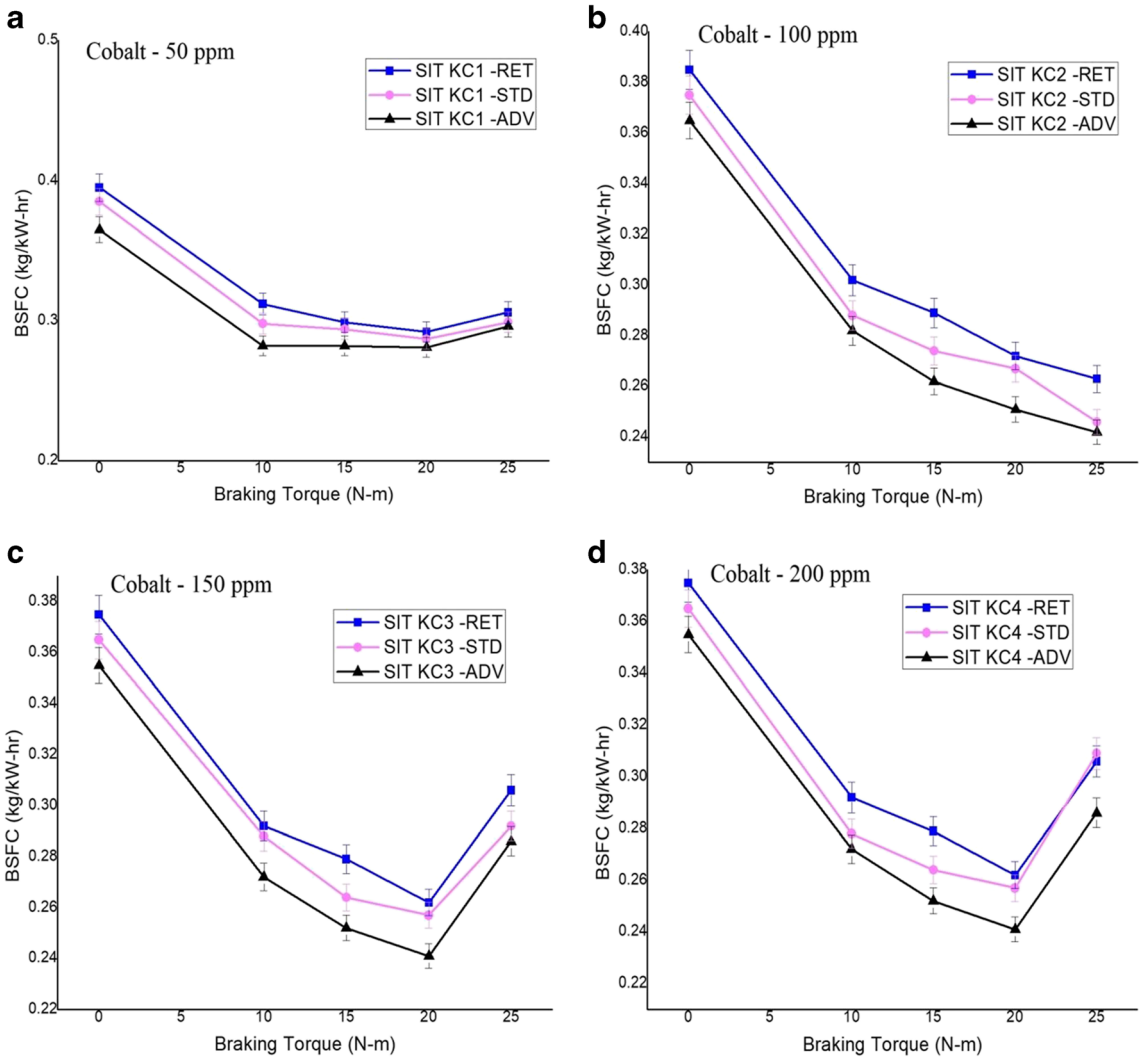

Fig. 14 Variation of braking torque Vs BSFC

5 Conclusions

The Kapok oil methyl ester biodiesel with nanoparticles was used in the base engine by varying the injection timings (IT). The nanoparticles dosage increased the thermal efficiency, in-cylinder pressure and HRR by improving the combustion process along with a drastic reduction of the emission characteristics when the IT was advanced and retarded.

➢ For the advanced IT, brake thermal efficiency (BTE) was 7.2% higher for the blend KC4 –ADV at standard IT (SIT) than the SIT. It is due to the presence of nanoparticles in the fuel and complete combustion process.
➢ When the IT was advanced, the brake specific fuel consumption of the blend SIT KC4 -ADV decreased by 21.23% compared with the 23 CAD bTDC because of the availability of nanoparticles within the fuel and shorter ID period.
➢ HRR and in-cylinder pressure in the blend SIT KC4 -ADV was higher by 5.09% and 5.72%, respectively, when correlated with the IT of 23 CAD bTDC due to the oxidization reaction within the fuel and complete combustion process.
➢ The hydrocarbon and carbon monoxide emissions in the blend SIT KC4 –ADV at advance IT showed a decrement of 37.86% and 41.66%, respectively, as compared with the SIT due to the oxidation reaction takes place and shorter ID period.
➢ The nitrogen oxides and carbon monoxide emissions for the blend SIT KC1 –RET at retarded IT decreased by 16.45% and 9.5%, respectively, when compared with SIT due to the shorter ID period, availability of oxygen within the fuel and less amount of fuel injected during the combustion process.

6 Summary of results

Figures 17 and 18 show the comparison result of advance and retard IT with standard IT.

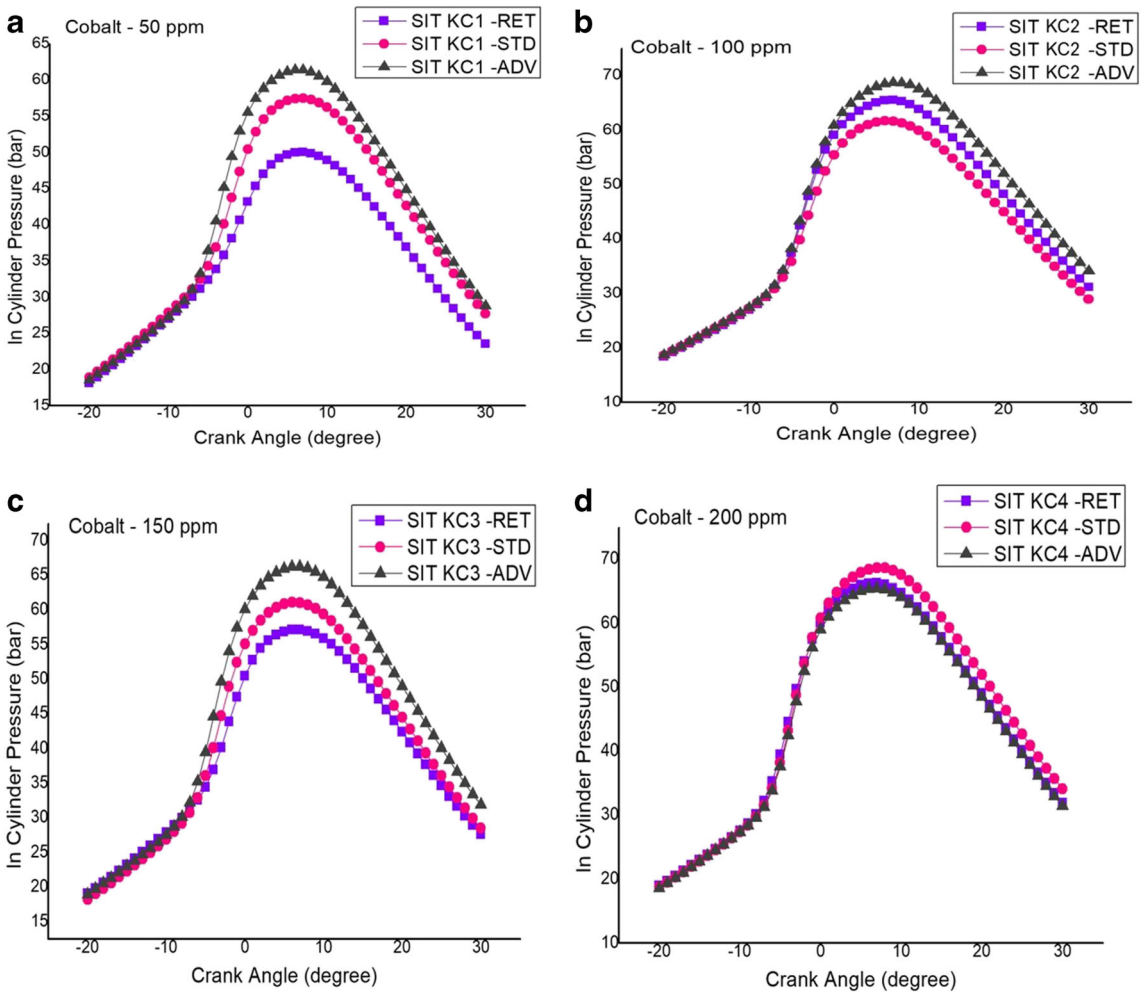

Fig. 15 Variation of Crank Angle Vs In cylinder pressure

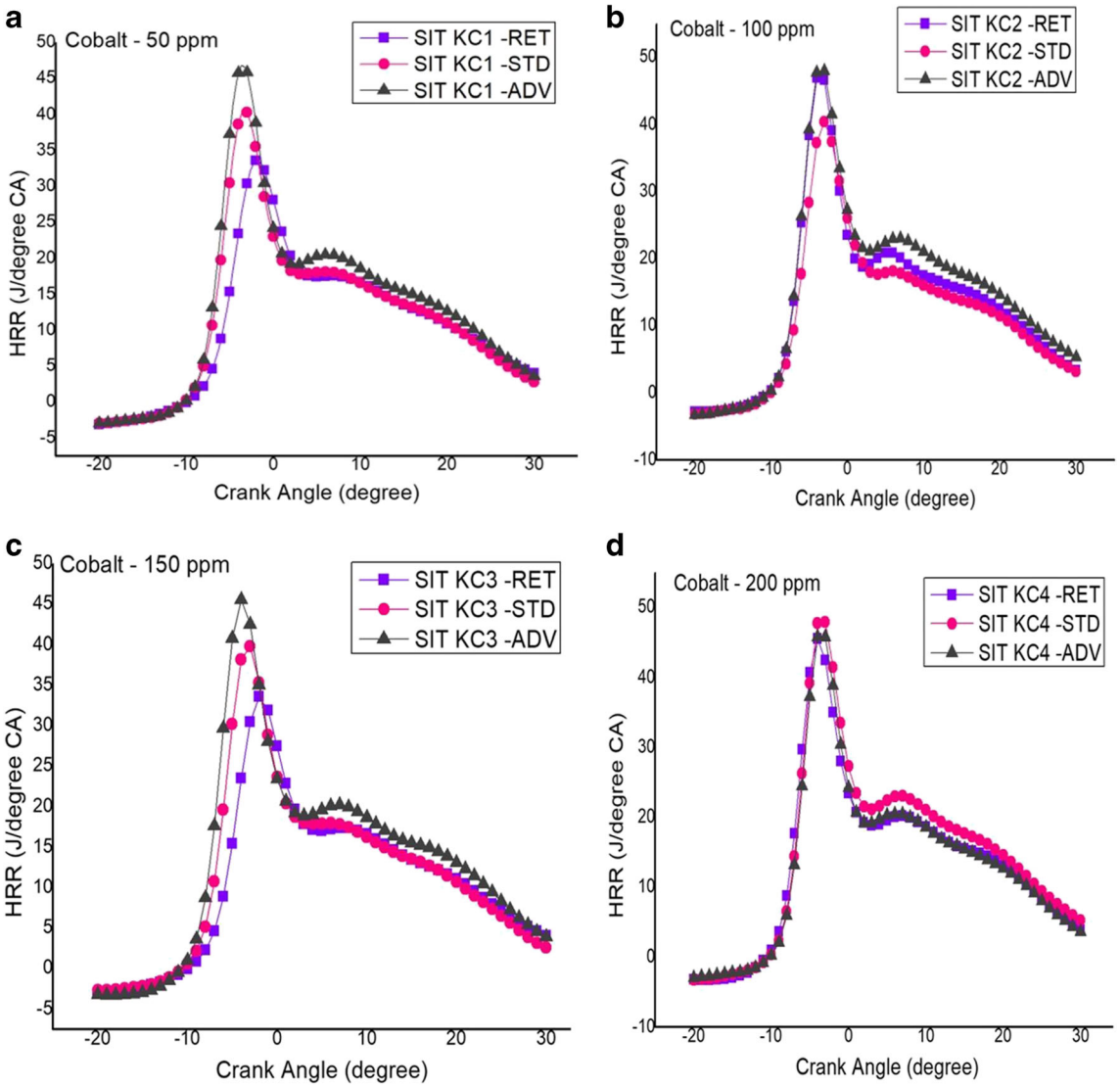

Fig. 16 Variation of Crank Angle Vs HRR

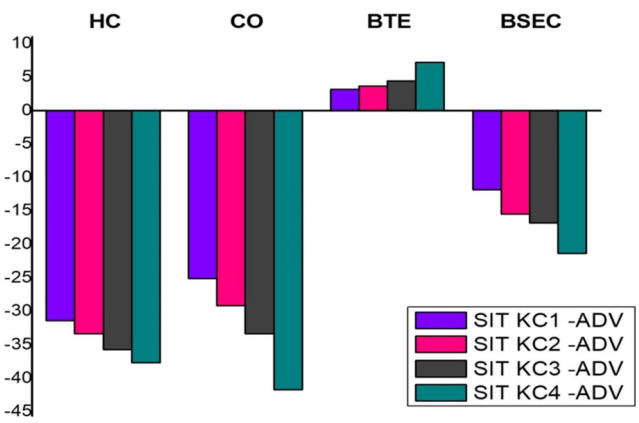

Fig. 17 Comparison of Advanced Injection Timing Vs Standard Injection Timing

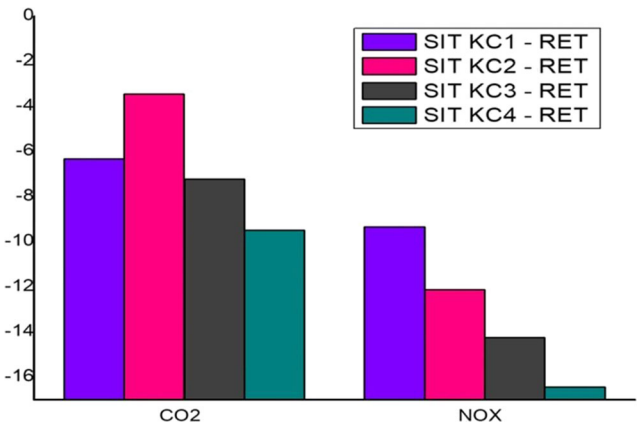

Fig. 18 Comparison of Retardation Injection Timing Vs Standard Injection Timing

Acknowledgements AICTE, the government of India for granting grants under modernization and elimination of obsolescence (AICTE), and management of the PSNA College of Engineering and Technology, Dindigul for providing a matching grant for the purchase of variable-compression ratio system (MODROB) are to be thanked by this corresponding author. The supervisor and the All-Indian Council for Technical Education (AICTE). In this rig the research work was carried out.

References

1. Bari S, Lim TH, Yu CW (2002) Effects of preheating of crude palm oil (CPO) on injection system, performance and emission of a diesel engine. Renew Energy 27:339–351. https://doi.org/10.1016/S0960-1481(02)00010-1
2. Deepanraj B, Lawrence P, Sivashankar R, Sivasubramanian V (2016) Analysis of pre-heated crude palm oil, palm oil methyl ester and its blends as fuel in a diesel engine. Int J Ambient Energy 37:495–500. https://doi.org/10.1080/01430750.2015.1004106
3. Namliwan N, Wongwuttanasatian T (2014) Performance of diesel engine using diesel B3 mixed with crude palm oil. Sci World J 2014. https://doi.org/10.1155/2014/531868
4. Subramaniam M, Solomon JM, Nadanakumar V et al (2020) Experimental investigation on performance, combustion and emission characteristics of DI diesel engine using algae as a biodiesel. Energy Rep 6:1382–1392. https://doi.org/10.1016/j.egyr.2020.05.022
5. Oni BA, Oluwatosin D (2020) Emission characteristics and performance of neem seed (Azadirachta indica) and Camelina (Camelina sativa) based biodiesel in diesel engine. Renew Energy 149:725–734. https://doi.org/10.1016/j.renene.2019.12.012
6. Temizer İ, Cihan Ö, Eskici B (2020) Numerical and experimental investigation of the effect of biodiesel/diesel fuel on combustion characteristics in CI engine. Fuel 270. https://doi.org/10.1016/j.fuel.2020.117523
7. Reza Miri SM, Mousavi Seyedi SR, Ghobadian B (2017) Effects of biodiesel fuel synthesized from non-edible rapeseed oil on performance and emission variables of diesel engines. J Clean Prod 142:3798–3808. https://doi.org/10.1016/j.jclepro.2016.10.082
8. Heidari-Maleni A, Gundoshmian TM, Karimi B et al (2020) A novel fuel based on biocompatible nanoparticles and ethanol-biodiesel blends to improve diesel engines performance and reduce exhaust emissions. Fuel 276:118079. https://doi.org/10.1016/j.fuel.2020.118079
9. Sivakumar M, Shanmuga Sundaram N, Ramesh Kumar R, Syed Thasthagir MH (2018) Effect of aluminium oxide nanoparticles blended pongamia methyl ester on performance, combustion and emission characteristics of diesel engine. Renew Energy 116:518–526. https://doi.org/10.1016/j.renene.2017.10.002
10. Saravanan A, Murugan M, Sreenivasa Reddy M, Parida S (2020) Performance and emission characteristics of variable compression ratio CI engine fueled with dual biodiesel blends of rapeseed and Mahua. Fuel 263:116751. https://doi.org/10.1016/j.fuel.2019.116751
11. Kumaravel ST, Murugesan A, Vijayakumar C, Thenmozhi M (2019) Enhancing the fuel properties of Tyre oil diesel blends by doping nano additives for green environments. J Clean Prod 240:118128. https://doi.org/10.1016/j.jclepro.2019.118128
12. How HG, Masjuki HH, Kalam MA, Teoh YH (2018) Influence of injection timing and split injection strategies on performance, emissions, and combustion characteristics of diesel engine fueled with biodiesel blended fuels. Fuel 213:106–114. https://doi.org/10.1016/j.fuel.2017.10.102
13. Zhang P, He J, Chen H et al (2020) Improved combustion and emission characteristics of ethylene glycol/diesel dual-fuel engine by port injection timing and direct injection timing. Fuel Process Technol 199:106289. https://doi.org/10.1016/j.fuproc.2019.106289
14. Harun Kumar M, Dhana Raju V, Kishore PS, Venu H (2020) Influence of injection timing on the performance, combustion and emission characteristics of diesel engine powered with tamarind seed biodiesel blend. Int J Ambient Energy 41:1007–1015. https://doi.org/10.1080/01430750.2018.1501741
15. Rajendran S (2020) Effect of antioxidant additives on oxides of nitrogen (NOx) emission reduction from Annona biodiesel operated diesel engine. Renew Energy 148:1321–1326. https://doi.org/10.1016/j.renene.2019.10.104
16. Huang J, Wang Y, Qin JB, Roskilly AP (2010) Comparative study of performance and emissions of a diesel engine using Chinese pistache and jatropha biodiesel. Fuel Process Technol 91:1761–1767. https://doi.org/10.1016/j.fuproc.2010.07.017
17. Valente OS, Pasa VMD, Belchior CRP, Sodré JR (2012) Exhaust emissions from a diesel power generator fuelled by waste cooking oil biodiesel. Sci Total Environ 431:57–61. https://doi.org/10.1016/j.scitotenv.2012.05.025
18. Can Ö (2014) Combustion characteristics, performance and exhaust emissions of a diesel engine fueled with a waste cooking oil biodiesel mixture. Energy Convers Manag 87:676–686. https://doi.org/10.1016/j.enconman.2014.07.066
19. Ong HC, Masjuki HH, Mahlia TMI et al (2014) Engine performance and emissions using Jatropha curcas, Ceiba pentandra and Calophyllum inophyllum biodiesel in a CI diesel engine. Energy 69:427–445. https://doi.org/10.1016/j.energy.2014.03.035
20. Chuah LF, Aziz ARA, Yusup S et al (2015) Performance and emission of diesel engine fuelled by waste cooking oil methyl ester derived from palm olein using hydrodynamic cavitation. Clean Techn Environ Policy 17:2229–2241. https://doi.org/10.1007/s10098-015-0957-2
21. Valente OS, Da Silva MJ, Pasa VMD et al (2010) Fuel consumption and emissions from a diesel power generator fuelled with castor oil and soybean biodiesel. Fuel 89:3637–3642. https://doi.org/10.1016/j.fuel.2010.07.041
22. Al-lwayzy SH, Yusaf T (2017) Diesel engine performance and exhaust gas emissions using microalgae Chlorella protothecoides biodiesel. Renew Energy 101:690–701. https://doi.org/10.1016/j.renene.2016.09.035
23. Tayari S, Abedi R, Rahi A (2020) Comparative assessment of engine performance and emissions fueled with three different biodiesel generations. Renew Energy 147:1058–1069. https://doi.org/10.1016/j.renene.2019.09.068
24. Shaafi T, Velraj R (2015) Influence of alumina nanoparticles, ethanol and isopropanol blend as additive with diesel-soybean biodiesel blend fuel: combustion, engine performance and emissions. Renew Energy 80:655–663. https://doi.org/10.1016/j.renene.2015.02.042
25. Mehta RN, Chakraborty M, Parikh PA (2014) Nanofuels: combustion, engine performance and emissions. Fuel 120:91–97. https://doi.org/10.1016/j.fuel.2013.12.008
26. Mirzajanzadeh M, Tabatabaei M, Ardjmand M et al (2015) A novel soluble nano-catalysts in diesel-biodiesel fuel blends to improve diesel engines performance and reduce exhaust emissions. Fuel 139:374–382. https://doi.org/10.1016/j.fuel.2014.09.008
27. Nadeem M, Rangkuti C, Anuar K et al (2006) Diesel engine performance and emission evaluation using emulsified fuels stabilized by conventional and gemini surfactants. Fuel 85:2111–2119. https://doi.org/10.1016/j.fuel.2006.03.013
28. Thiyagarajan S, Sonthalia A, Edwin Geo V et al (2020) Effect of manifold injection of methanol/n-pentanol in safflower biodiesel fuelled CI engine. Fuel:261. https://doi.org/10.1016/j.fuel.2019.116378

29. Yang WM, An H, Chou SK et al (2013) Emulsion fuel with novel nano-organic additives for diesel engine application. Fuel 104:726–731. https://doi.org/10.1016/j.fuel.2012.04.051
30. Sadhik Basha J, Anand RB (2014) Performance, emission and combustion characteristics of a diesel engine using carbon nanotubes blended Jatropha methyl Ester emulsions. Alexandria Eng J 53: 259–273. https://doi.org/10.1016/j.aej.2014.04.001
31. Ayhan V, Çangal Ç, Cesur İ et al (2020) Optimization of the factors affecting performance and emissions in a diesel engine using biodiesel and EGR with Taguchi method. Fuel 261. https://doi.org/10.1016/j.fuel.2019.116371
32. Nikzadfar K, Shamekhi AH (2019) Investigating a new model-based calibration procedure for optimizing the emissions and performance of a turbocharged diesel engine. Fuel 242:455–469. https://doi.org/10.1016/j.fuel.2019.01.072
33. Rajesh Kumar B, Saravanan S (2016) Effects of iso-butanol/diesel and n-pentanol/diesel blends on performance and emissions of a di diesel engine under premixed LTC (low temperature combustion) mode. Fuel 170:49–59. https://doi.org/10.1016/j.fuel.2015.12.029
34. Chen Z, Liu J, Han Z et al (2013) Study on performance and emissions of a passenger-car diesel engine fueled with butanol-diesel blends. Energy 55:638–646. https://doi.org/10.1016/j.energy.2013.03.054
35. Li L, Wang J, Wang Z, Liu H (2015) Combustion and emissions of compression ignition in a direct injection diesel engine fueled with pentanol. Energy 80:575–581. https://doi.org/10.1016/j.energy.2014.12.013
36. Choi B, Jiang X, Kim YK et al (2015) Effect of diesel fuel blend with n-butanol on the emission of a turbocharged common rail direct injection diesel engine. Appl Energy 146:20–28. https://doi.org/10.1016/j.apenergy.2015.02.061
37. Vedharaj S, Vallinayagam R, Yang WM et al (2014) Effect of adding 1,4-Dioxane with kapok biodiesel on the characteristics of a diesel engine. Appl Energy 136:1166–1173. https://doi.org/10.1016/j.apenergy.2014.04.012
38. Rajesh Kumar B, Saravanan S, Sethuramasamyraja B, Rana D (2017) Screening oxygenates for favorable NOx/smoke trade-off in a DI diesel engine using multi response optimization. Fuel 199: 670–683. https://doi.org/10.1016/j.fuel.2017.03.041
39. Krishnamoorthy R, Asaithambi K, Balasubramanian D, Murugesan P, Rajarajan A (2020) Effect of Cobalt Chromite on the Investigation of Traditional CI Engine Powered with Raw Citronella Fuel for the Future Sustainable Renewable Source. SAE Technical Paper 2020-28-0445, 2020. https://doi.org/10.4271/2020-28-0445
40. Elumalai PV, Annamalai K, Dhinesh B (2019) Effects of thermal barrier coating on the performance, combustion and emission of DI diesel engine powered by biofuel oil–water emulsion. J Therm Anal Calorim 137:593–605. https://doi.org/10.1007/s10973-018-7948-6
41. Uslu S, Ayd M (2020) Effect of operating parameters on performance and emissions of a diesel engine fueled with ternary blends of palm oil biodiesel / diethyl ether / diesel by Taguchi method. Fuel 275:117978. https://doi.org/10.1016/j.fuel.2020.117978
42. Balusamy T, Marappan R (2010) Effect of injection time and injection pressure on CI engine fuelled with methyl ester of Thevetiaperuviana seed oil. Int J Green Energy 7(4):397–409
43. Harish V, Venkataramanan M (2016) Effect of Al2O3 nanoparticles in biodiesel- diesel-ethanol blends at various injection strategies: performance, combustion and emission characteristics. Fuel 186:176–189. https://doi.org/10.1016/j.fuel.2016.08.046
44. Sayin C, Gumus M, Canakci M (2010) Effect of fuel injection timing on the emissions of a direct-injection (DI) diesel engine fueled with canola oil methyl ester diesel fuel blends. Energy Fuel 24(4):2675–2682
45. Channapattana SV, Pawar Abhay A, Kamble Prashant G. Investigation of DI-CI four stroke VCR engine at different fuel injection timing using bio-fuel derived from nonedible oil source as a fuel. Biofuels Taylor &Francis Group LLC; 2016. https://doi.org/10.1080/17597269.2016.1187540. ISSN: 1759–7269 (Print) 1759–7277
46. Ganapathy T, Gakkhar RP, Murugesan K (2011) Influence of injection timing on performance, combustion and emission characteristics of Jatropha biodiesel engine. Appl Energy 88:4376–4386
47. Nanthagopal K, Ashok B, Raj RT (2016) Influence of fuel injection pressures on Calophyllum inophyllum methyl ester fuelled direct injection diesel engine. Energy Convers Manag 116:165–173
48. Elumalai PV, Nambiraj M, Parthasarathy M et al (2021) Experimental investigation to reduce environmental pollutants using biofuel nano-water emulsion in thermal barrier coated engine. Fuel 285:119200. https://doi.org/10.1016/j.fuel.2020.119200
49. Elumalai PV, Dhinesh B, Parthasarathy M et al (2020) An experimental study on harmful pollution reduction technique in low heat rejection engine fuelled with blends of pre-heated linseed oil and nano additive. J Cleaner Prod:124617. https://doi.org/10.1016/j.jclepro.2020.124617